

Boron Doped Graphene as a Negative Electrode Additive for High Performance Lead-Acid Batteries

A Project Report Submitted

as part of the requirements for the degree of

MASTER OF SCIENCE

By

Udita Bhattacharjee

(Roll No. CY16MSCST11027)

Under the supervision of

Dr. Surendra Kumar Martha



to the

DEPARTMENT OF CHEMISTRY

INDIAN INSTITUTE OF TECHNOLOGY HYDERABAD

INDIA

MAY, 2018

Declaration

I hereby declare that the matter embodied in this report is the result of investigation carried out by me in the Department of Chemistry, Indian Institute of Technology Hyderabad under the supervision of Dr. Surendra Kumar Martha.

In keeping with general practice of reporting scientific observations, due acknowledgement has been made wherever the work described is based on the findings of other investigators.



Signature of the Supervisor

Dr. Surendra K. Martha, Ph.D.
Assistant Professor
Department of Chemistry
Indian Institute of Technology Hyderabad
Kandi, Sangareddy 502 285, Telangana, India

Udita Bhattacharjee

(Signature)

UDITA BHATTACHARJEE

(– Student Name –)

CY16MSCST11027

(Roll No)

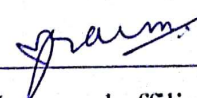
Approval Sheet

This thesis entitled Boron Doped Graphene as a Negative Electrode Additive for High Performance Lead-Acid Batteries by Udit Bhattacharjee is approved for the degree of Master of Science.



-Name and affiliation-

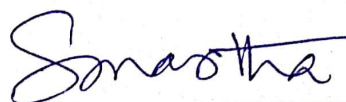
Examiner



Dr. Praveen
Meduri

-Name and affiliation-

Examiner



Dr. Surendra K. Martha, Ph.D.
Assistant Professor

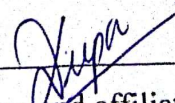
-Name and affiliation-

Adviser

Department of Chemistry
Indian Institute of Technology Hyderabad
Kandi, Sangareddy 502 285, Telangana, India

-Name and affiliation-

Co-Adviser



-Name and affiliation-

Chairman

Acknowledgements

First of all, I would like to express my sincere gratitude to my research supervisor **Dr. Surendra Kumar Martha** for being a continuous support during my M.Sc. course work and research, for his knowledge, patience and endearing behavior. His guidance motivated me during my research and helped me while writing my thesis. Throughout, my whole M.Sc. he counselled me a lot towards further career opportunities.

Apart from my advisor, I would like to thank all the faculty members of Department of Chemistry, Indian Institute of Technology Hyderabad for sharing their knowledge with us and helping us learn better. I would also like to show my sincere towards all the lab technicians of Department of Chemistry.

I would thank my examiners Dr. M. Deepa and Dr Praveen Meduri for evaluating my project.

My sincere thanks to my mentor Mr. Naresh Vangapally, PhD Scholar who helped me and equally contributed to this work.

I would like to thank NED Energy Ltd., our industrial partner.

I would like to thank my family: my parents Mr. Dipankar Bhattacharjee and Mrs. Jayasree Bhattacharjee, my younger sister Ms. Malyosree Bhattacharjee and Mr. Parth Gupta for constantly supporting me throughout the ups and downs faced by me during this project as well as in life.

I would also like to thank my friends: Sakshi, Ankita, Poulomi, Madhushri, Alisha, all my labmates and classmates for keeping me motivated all throughout and helping me whenever it was required.

Dedicated to

To my Family and Friends

Abstract

Lead-acid battery remains the most successful battery system ever developed. Although lead-acid battery designs have been optimized in the past in several different ways, there are still certain new challenges faced by lead-acid battery designers, as additional failure modes become evident in various end-uses. In this work we have studied the effect of Boron doped graphene as an additive for the negative electrode in lead acid battery. B-doped graphene synthesized from the solvothermal method. Boron doping confirmed by the different characterization methods. X-ray photoelectron spectroscopy (XPS) measurement confirms the atomic level of boron (3.11 %) is doped into the boron doped graphene. Here we have systematically investigated the various percentages of the Boron doped graphene (0, 0.25, 0.5 and 1wt. %) additive added to the negative active material (NAM). Besides this study involves optimized the additive w.r.t negative active material and percentage of boron in boron doped graphene, it is found that 0.25 wt.% B-doped graphene additive in negative electrode which contains around 3% of Boron doping in the graphene shows optimum results. Boron doped graphene additive shows the impressive electrochemical performance in first discharge capacity, ~80% increases the capacity compared to the without born doped additive. An increase in capacity by 15-20% at lower C rates and the increase in capacity is almost double at higher C rates which indicates that this modified additive can be used for potential application in lead acid battery. Charge transfer dependent on the holes present the boron doped graphene and significant changes in the electronic structure of the graphene. Our results confirm the boron doping onto the graphene lattice it gives superior electrochemical performances and high rate partial charge cycling in lead acid batteries negative electrode additive.

Contents:

CHAPTER 1 Introduction to Lead-Acid Battery

1.1. Components of a lead acid battery	9
1.2. Working Principle.....	10
1.3. Fabrication and Assembly of battery.....	13
1.4. Secondary Reactions.....	17
1.5. Problems Associated with Lead Acid Battery.....	18
1.6. Applications of LAB.....	23
1.7. Advancements in Lead Acid Battery.....	24
1.8. Various carbon compounds used as an additive.....	30
References.....	33

CHAPTR 2 Nano Structured Reduced Graphene Oxide (RGO) Coated TiO₂ as a Negative Electrode Additive for Advanced Lead acid Batteries

2.1 Introduction to Our Approach.....	37
2.2. Chemicals and Reagents.....	39
2.3 Experimentals.....	39
2.3.1 Synthesis of Graphene Oxide (GO) by Modified Hummer's Method.....	39
2.3.2 Synthesis of Thermally reduced Graphene Nanosheets.....	41
2.3.3 Synthesis of Boron Doped Graphene Nanosheet.....	42
2.2.4 Structural Physical characterizations	42
2.2.5 Fabrication and Assembly of battery electrodes.....	42
2.2.6 Electrochemical measurements.....	44
2.4. Results and Discussions	
2.4.1. Structural Characterization:	45
2.4.2. Morphology Studies.....	47
2.4.3. X-ray Photoelectron Spectroscopy	47

2.4.4. Thermal Gravimetric Analysis.....	49
2.4.5. Electrochemical Characterization.....	50
Summary of the Work.....	55
References.....	56

Chapter 1: Introduction to Lead Acid Batteries

Lead Acid Battery was invented by Raymond Gaston Plante in 1859 [1]. It is the first discovered rechargeable battery [1-3] and still occupies almost 50% of market of the commercially available batteries. Lead-acid battery production and use continue to grow because of its newer applications such as starting, lighting, and ignition, telecommunication, power tools, as a power source for mining and material-handling equipments and even in hybrid-electric vehicles [3-7]. The widespread use of the lead-acid battery in many designs, sizes, and system voltages is reflected by its low price and the ease of manufacture.

1.1. Components of a lead acid battery:

The lead acid battery operates on simple lead acid battery electrochemistry. The components of a lead acid battery include an anode, a cathode, electrolyte and a separator (Fig.1). The anode which is the negative electrode in a lead acid battery is composed of spongy lead (Pb). The cathode or positive electrode of this battery is made up of Lead Dioxide (PbO₂). Both the plates are immersed in an electrolyte which is an aqueous solution of H₂SO₄. The composition of the electrolyte is 4.5 M H₂SO₄. The necessary conditions for an effective electrolyte is highly ionically conducting but electronically insulating. The aqueous 5 M H₂SO₄ solution shows its maximum conductivity. 4.5 M H₂SO₄ in the battery during charge-discharge is optimized at 5M. A separator is used in order to prevent the short circuiting of the cell but the necessary condition being permeability of the electrolyte through the separator. The separators generally used in the lead acid battery are polymeric separator, absorptive glass mat (AGM) separator [7-9].

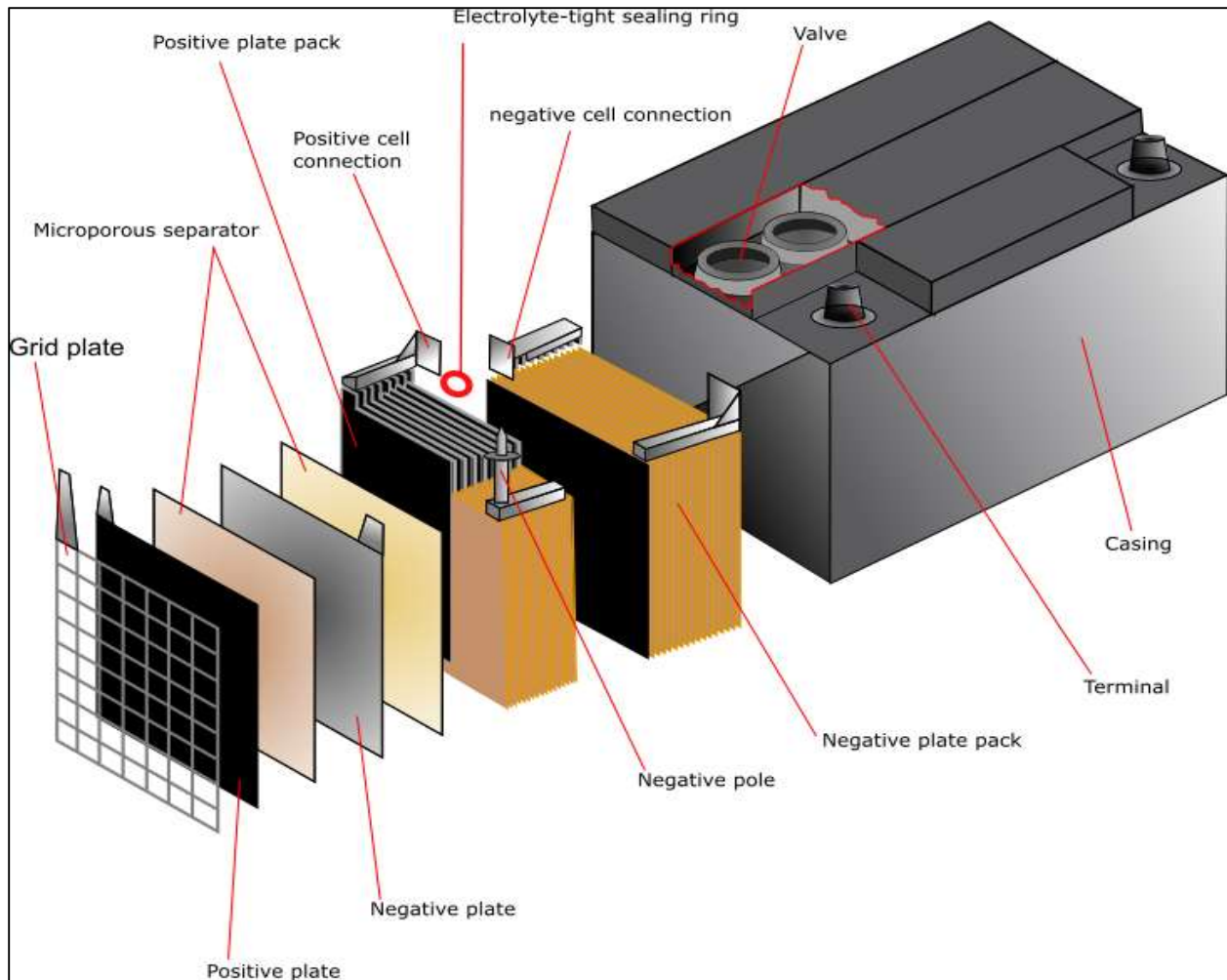


Figure 1. Components of a lead-acid battery

1.2. Working Principle of Lead-Acid Battery

During the discharging process:

During the process of discharging the electrolyte i.e. Sulfuric acid is consumed and the solid product is formed which is insulating in nature i.e. Lead (II) sulfate.

At the positive electrode or cathode, the lead dioxide, PbO_2 (IV) reduced to lead sulfate $PbSO_4$ (II) during the process of discharge.



At the negative electrode or anode the spongy lead metal, Pb (0) is oxidized to lead sulfate, PbSO₄ (II) during this process.



The total redox reaction taking place in the process of discharge is



The open-circuit-voltage of a lead-acid cell is about 2.06 V. When circuit is completed electrons flow from negative electrode to the positive electrode and the electric current is generated in the opposite direction. Thus, the redox reaction gives out energy which is converted into electrical energy and is used by various systems. The discharge process is shown in Fig.2.

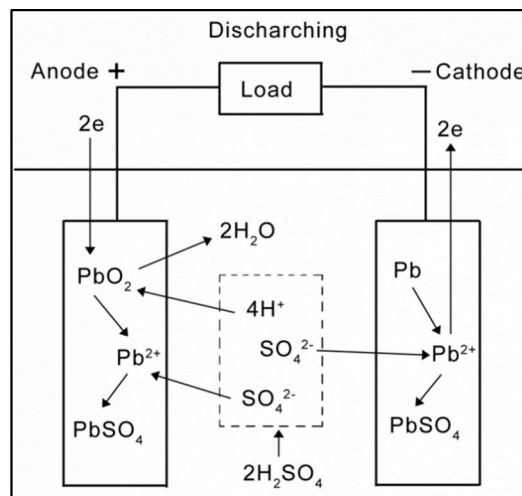


Figure 2: Schematic diagram of Discharging of lead acid battery

During the process of charging:

The cell takes up electrical energy provided and converts it into chemical energy and results into the following conversions. Schematic diagram of charging of lead acid battery is shown in Fig.3.

At the negative electrode, the lead sulfate, PbSO_4 that is formed during discharge is reversed back to spongy lead, Pb



At the positive electrode or cathode, the lead sulfate, PbSO_4 crystals formed are converted back to lead dioxide, PbO_2



The total reverse reaction during charging is as follows



Here, the electrical energy is consumed and the insulating solid lead sulfate that was formed during the discharge was converted back to the non-insulating spongy lead and lead oxide [10-11].

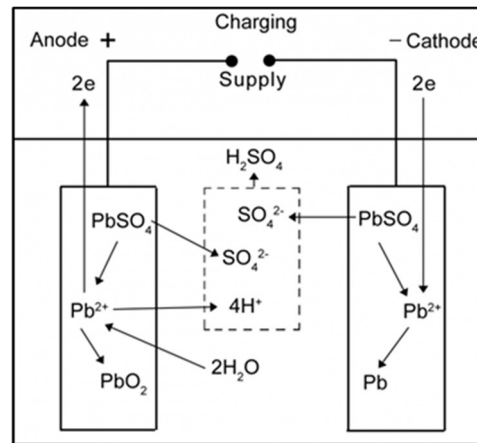


Figure 3: Schematic diagram of charging of lead acid battery

1.3. Fabrication and Assembly of cells and Batteries

Several cells connected in series to obtain Lead Acid Batteries. To obtain high capacity similar electrodes are connected in parallel. The cell fabrication process involves various steps as discussed below.

Grid Formation: The grid for the electrodes are made using an alloy of spongy lead and other conducting metals. The purpose of the grid is to provide mechanical support for the active material of the respective electrodes. It also acts as a current collector as it is electrically conducting in nature. It should be free from corrosion attack. Additives such as Al, Sn, Ca in small percentages are used to improve corrosion stability of lead in acidic environment. Al, Sn and Ca are more conducting in nature as compared to lead and are also harder metals Thus, they are used for stiffening of grid and also for corrosion resistance, the added advantage being their least participation in the cell reaction. The amount of Ca that is used for corrosion stability is around 0.03 – 0.05% and that of Sn used is 0.25 – 2%. Grid is a rectangular framework of horizontal and vertical wires. An advanced commercially used form of this grid is tubular grid.

Paste Mixing: In this process the active material i.e. Lead oxide which is a mixture of Pb and PbO is mixed with lignin, Barium sulfate, sulfuric acid and other expanders and additives and then mechanically mixed in a grinding machine. The organic expanders provide porosity in the material and the fibers provide better mechanical strength of the pastes. Barium sulfate having common ion with lead sulfate is thought to decrease the size of the lead sulfate formed.

Besides, positive plate is mixed with 25 % of Pb_3O_4 to improve the formation efficiency and conductivity of the paste.

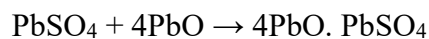
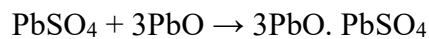
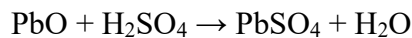
While mixing the specific condition of temperature and amount of sulfuric acid is maintained in order to maintain a certain viscosity of the paste and thus the final density of the plates. In general, our positive paste density is 4.4 g/cc and negative paste density is 4.2 g/cc.

Pasting: Pasting is a process in which the paste prepared for the active material of electrode is pasted into the grids or current collectors. The paste is pressed using hand trowel or machine. The machine method may be of two types. First one being fixed orifice paster in which the paste is given from both the directions and then pressed. The second one is a belt paster in which the paste is provided from one direction and then pushed towards the other direction.

Drying: The plates are acid washed in 1.1 M H₂SO₄ after pasting. This process is call prickling. After prickling the electrodes are kept for drying at temperatures between 50-100 °C [8,12,14].

Curing:

Curing is necessary for the conversion of leady oxide to the basic lead sulfates from which the formation cycles results in the electrochemically active lead and lead dioxide. Curing process makes active materials are in good contact with grid. The process involves treating of the plates at ~60°C in the presence of a humidity of around 70% for 24 h. After curing the tetrabasic lead sulfate, 4BS (4PbO. PbSO₄) and tribasic lead sulfate, 3BS (3PbO. PbSO₄) are produced and the free lead content is reduced. The reactions that take place during curing are [13, 16]:



Assembly: After curing the positive and negative electrodes are stacked alternatively by placing a separator between them. A separator may be made of some organic polymer based on polyethylene or polyvinyl chloride or Absorbent Glass Mat (AGM). All the positive electrodes are soldered together to give a single positive terminal and similarly all the negative electrodes are soldered together to give the negative terminal of the battery. Thus, many cells are combined in series to give a battery. This whole assembly of electrodes and separators is put into a case. Then the case is filled with the electrolyte i.e. 4.5 M H_2SO_4 . Flowchart showing the preparation of electrodes of lead acid battery is presented in Fig.4.

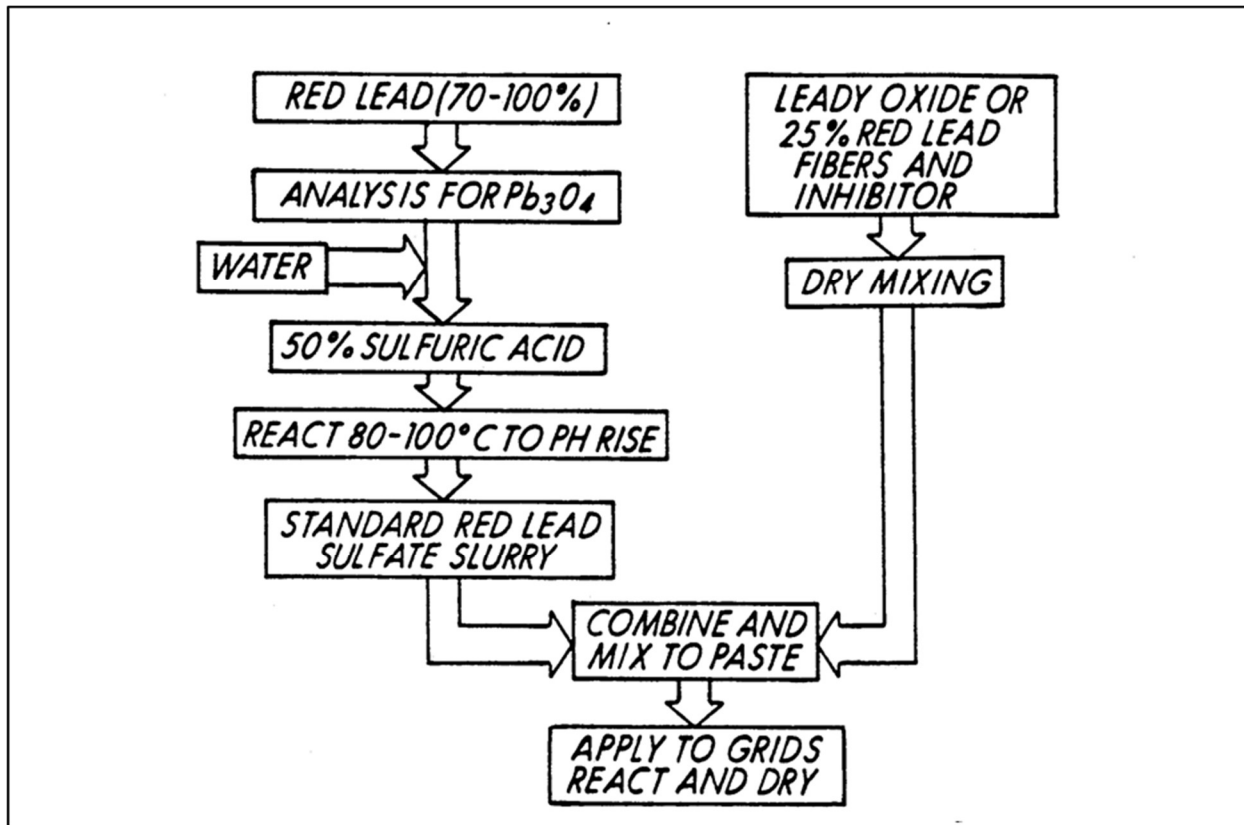


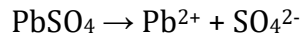
Figure 4: Flowchart showing the preparation of electrodes of lead acid battery [15].

Soaking: The electrodes are needed to be soaked in aqueous sulfuric acid so that the acid reaches the pores of the electrode through capillary action. In this process, acidic environment is induced

by the acidic electrolyte and the basic lead sulfate is converted to neutral lead sulfate which is non-conducting in nature.



PbSO_4 remains in a partly dissolved state in the sulfuric acid electrolyte.



Formation: After the soaking, formation charge is provided to the electrode plates. The conduction of electrons takes place through the grid. In the negative electrode, the dissolved Pb^{2+} present in the interface between the grid and electrolyte takes up electron and gets converted to Pb metal and active material which is the primary electrochemical reaction in the battery. In the positive electrode the neutral lead sulfate is converted to the lead dioxide which is the active material for the positive plate of working lead acid battery.

Sealing and Testing: The battery is sealed in the end by covering the case. Vent caps are provided at the top of case to release gasses evolve during charge. The batteries are tested to obtain electrical performances. The type of testing depends on the type of application the battery is about to exhibit.

Various types of charging methods are involved: Constant Current (Current passed is kept constant at different current rates, not used widely only laboratory purposes), Constant Potential (The voltage is maintained to be constant until the battery is called on to discharge, used for on road vehicles, telephone and power supply), Taper Charging (modified version of constant potential), Pulse charging (mainly used for traction application, the charging from the terminals is periodically removed and open circuit voltage is measured), Trickle Charging (Constant current charging at lower C-rates like C/100, used to maintain the battery in fully charged state), Float

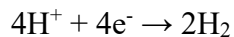
charging (Constant Potential charging at lower rates to ensure fully charged state of the battery, used for SLI batteries) and Rapid charging [17-18].

1.4. Secondary Reactions:

Many side reactions take place alongside the primary redox reaction whose evolved energy is converted to the electrical energy. The main reaction among them is that of splitting of water. This involves two steps, hydrogen evolution at negative electrode and oxygen evolution at the positive electrode. This happens because the potential for the water splitting reaction is 1.23 V.

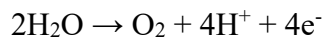
Hydrogen Evolution:

Hydrogen evolution takes place in negative electrode due to the overpotential.

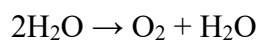


Oxygen Evolution:

With the hydrogen evolution in the negative electrode simultaneous oxygen evolution takes place at the positive electrode.



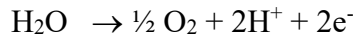
Thus, the overall reaction taking place during the decomposition of water can be given as



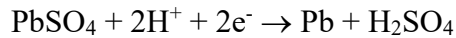
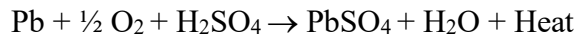
This splitting of water is one of the problems associated with Lead Acid Batteries [19-20]. Attempts have been made to solve this problem and Valve Regulated Lead Acid (VRLA) battery. They check the evolution of oxygen but the hydrogen gas is evolved at the negative electrode. The

mechanism for this explained by oxygen cycle according to which the oxygen produced at the positive electrode combines at the negative plate as given bellow,

At the positive plate:



At the negative plate:



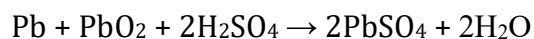
Thus, they are maintenance free batteries [28].

1.5. Problems associated with lead acid batteries:

Even though Lead acid batteries is optimized in all direction but still there are many issues still remain unresolved. Some of the most important problems associated with lead-acid batteries are:

Irreversible Sulfation of the active mass of electrodes:

This phenomenon involves the formation of lead sulfate in an irreversible manner over the active material of both the electrodes. During the process of discharge, the crystalline lead sulfate is formed as a result of both the electrode reactions. The spongy lead metal in the negative electrode is oxidized to solid insulating lead sulfate and similarly the lead dioxide in the positive plate is also reduced to solid mass of lead sulfate. Overall electrochemical reaction showing the formation during the discharge process is given bellow,



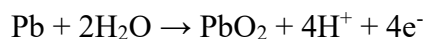
Since lead sulfate is formed as a discharged product, the efficiency of the battery is dependent on the reversibility of the process of formation and deformation of the lead sulfate. Moreover, this problem of irreversible sulfation is more likely seen in the negative plate. The larger crystals of lead sulfate get embedded into the pores of the spongy lead structure in the negative electrode and thus lose its reversibility. Thus, this makes the lead acid battery less efficient and causes its ageing [28].

Low Utilization of Active Material:

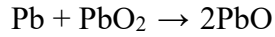
The irreversible formation of lead sulfate takes place on the surface both positive and negative electrodes of lead acid battery. Lead sulfate is insulating in nature electrically. It is a solid crystalline mass which forms a protective layer or coating over the electrode surface. Thus, all the active mass of the electrode cannot be utilized in the further working of the battery. This protective layer acts as a barrier in the smooth cycling of a lead acid battery. This results in the low utilization of the active mass of the electrodes [21-22].

Grid Corrosion at positive plate in LAB:

Grid corrosion is one of the main causes behind the ageing of lead acid batteries and also ultimately causes the natural death of these batteries. Positive electrode grid undergoes corrosion due to the formation of an intermediate oxide layer between the grid and the active material. Lead and Lead Dioxide cannot exist simultaneously in contact with one another. At higher potentials of the positive electrode the lead metal is oxidized to lead dioxide which is not a stable layer.

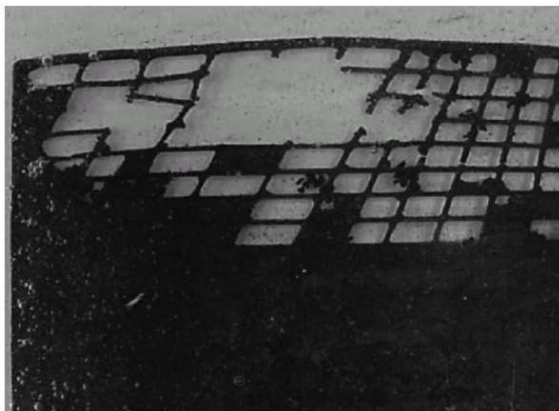


These further reacts with the remaining lead metal to give a lead oxide layer which is an electrochemically inactive form.

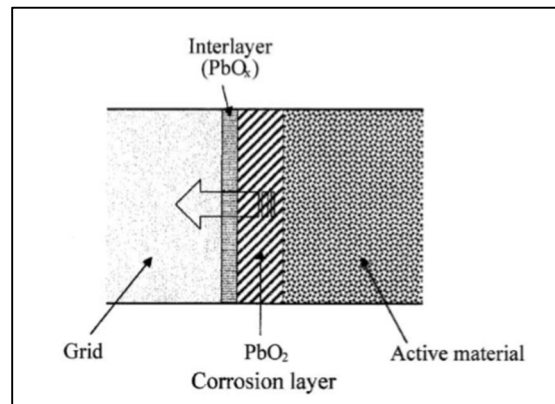


Higher lead oxides are also formed with various configurations, PbO_x .

Thus, this oxide layer when comes in contact with the acid electrolyte causes the formation of PbSO_4 . The $\text{PbO}_2/\text{PbO}_x$ corrosion layer gradually penetrates the grid and causes disruption of the grid wiring and the active material also gets shredded from the grid as shown in fig 5(b). This process occurs slowly like a solid state reaction. The contact between the active material and the current collector is also lost [23-24] causing premature failure.



(a)



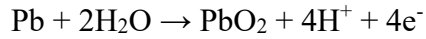
(b)

Figure 5: (a) Corroded grid (b) Schematic diagram of grid corrosion

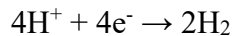
Water loss in LAB:

Water loss is one of the problems which gives rise to the need for maintenance of lead acid batteries and thus, make them less efficient for industrial usage. Water loss occurs due to the combined

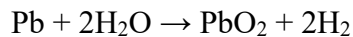
effects of two secondary reactions taking place during the working of lead acid batteries. The first reaction being the grid corrosion reaction taking place in the positive plate.



The second reaction that contributes to the phenomenon of water loss is the hydrogen evolution in the negative electrode.



Overall reaction for water loss can be given as



The water loss has to be kept minimum, otherwise the electrolyte becomes concentrated, the volume of electrolyte decreases and loses the conductivity of higher order and causes the battery capacity fade followed by malfunctioning [30].

Acid Stratification:

The stratification of acidic electrolyte in lead acid batteries occur due to the fact that electrolytes take part in the electrode reactions while charge and discharge. When the battery is discharged, SO_4^{2-} are consumed by the electrodes and water is also produced at the positive electrode. Thus, the specific gravity of the electrolyte near the electrodes decreases and hence becomes less dense near the electrode and above that level. At the end of discharge, the concentration of the electrolyte becomes denser in the bottom part of the battery. Thus, the uniformity of the electrolyte can be attained very slowly through diffusion. During recharging the SO_4^{2-} is released and water is also consumed in the positive electrode. The concentration of the acid near the electrodes increases and due to high specific density, the concentrated acid comes downward. The acid concentration at the

bottom increases and thus, stratifies. During charge-discharge cycling, the bottom part of the battery becomes denser in electrolyte concentration and the upper part becomes diluted. Thus, the optimum concentration for the electrolyte becomes disturbed. As a result of this stratification, the active material in the upper part of the electrodes is less utilized due to the lower concentration of the acid in the same. The same is shown in figure 6 [25-28].

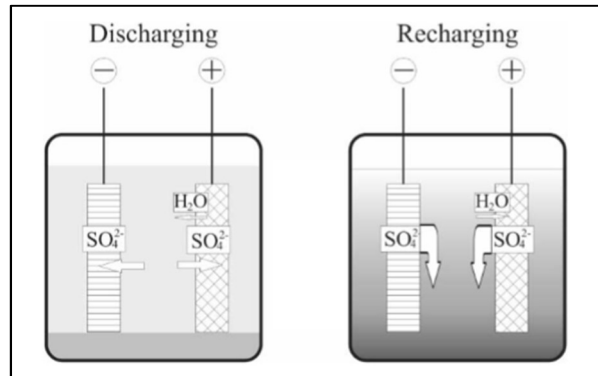


Figure 6: Acid Stratification while charge and discharge of lead acid batteries

This stratification problem can be reduced and mixing of the electrolyte can be achieved by using very fine fibers in the AGM separator. This increases the porosity of the separator and thus induces high capillary action. Thus, ensures even mixing of the electrolyte and makes it less stratified. Gelled electrolyte batteries can also be used for this purpose [29].

Hydrogen evolution, oxygen evolution, grid corrosion are the reactions which occur in open circuit voltage and result into the self-discharge of lead acid batteries.

Low Energy Density of LABs:

Lead Acid Batteries are heavier than most other rechargeable batteries discovered and commercially available. Lead is a heavy metal having molecular weight 207 g/mol and thus, the compounds of lead are also heavier. The specific energy of these batteries is low ~30 Wh/kg

compared to other batteries such as lithium ion batteries (~200 Wh/kg) . The specific capacity of these batteries is also low (~100 mAh /g) though it has a good cycling stability. This is one of the major drawback of LAB and makes them less efficient in competition to the other batteries.

Some other problems associated with lead acid batteries involve the leakage of its acid electrolyte through the sealed lid of the battery container, the poisonous nature of lead as a metal towards the environment and the living race and also the risk involved in its usage. Due to heavy weight of the lead acid batteries it cannot be used as an energy storage for light weight portable electronic devices. Besides, use of aqueous sulfuric acid as an electrolyte is not safe for applications such in mobile devices as there may be cases of acid spilling [8, 14].

1.6. Applications of lead acid batteries:

The lead acid battery market condition from 2014 to 2018 can be seen in the form of this bar graph [31]:

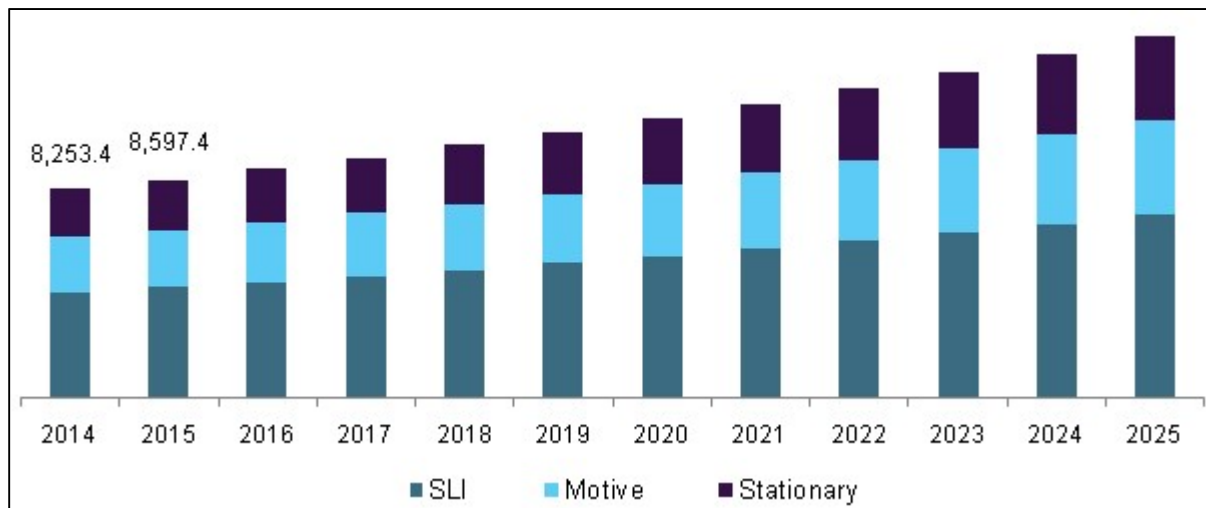


Figure 7: Survey on commercial usage of lead acid batteries from 2014-2025 [31]

Low cost and reliable performance is anticipated to drive the growth in the future. But high lead content, low energy density of the product can harm the environment and is expected to restrain growth. The emergence of alternative batteries like lithium ion batteries can affect this growth.

Lead acid batteries are one of the widely used rechargeable batteries industrially [8] since the time it was invented. Some of the applications are mentioned below [32-38]:

<u>Small energy storage</u>		<u>Industrial usage</u>		
Traction	Special	Traction	Stationary	Special
Golf cart, Off-road vehicles, On-road vehicles.	Emergency lighting, Alarm signals, Photovoltaic Sealed cells (for tools, instruments, electronic devices, etc.)	Mine locomotives, Industrial trucks, large electric vehicles	Switch gear Emergency lighting Telecommunication Railway signals Uninterrupted power supply Photovoltaics Load leveling and energy storage	Submarines Ocean buoys

1.7. Advancements in lead acid batteries:

Since its invention, LAB has been tried by many to improve the performance and efficiency of these batteries. The main reasons behind the less efficiency of these batteries were taken into account and those were tried to be mitigated.

From the beginning, it served to be one of the best rechargeable batteries which served the purpose of energy storage for stationary applications but had its limitation towards portability [39-40].

VRLA batteries i.e. the valve regulated lead acid batteries came into the scenario in the 1950s as an advanced form of the lead acid batteries. These batteries were a parallel to the rechargeable Ni-Cd batteries developed at that time which replaced lead acid batteries in the portable batteries. These batteries provided a route for the utilization of the oxygen gas evolved at the positive electrode as a result of secondary reactions through an internal oxygen cycle mentioned earlier. It also immobilized electrolyte by silica infused electrolyte. Then in 1970s a change into the scenario came when fine fiber absorptive glass mat was introduced so that the porosity and thus the problem of acid stratification was sorted and also the electrolyte was absorbed which further solved the problem of acid leakage from lead acid batteries. These also satisfied the need of sealed lead acid batteries though they cannot be completely sealed and some space should be left for the hydrogen gas to escape as the hydrogen gas evolution is a procedure which cannot be stopped to occur. But these made the portability of lead acid batteries possible and the first portable lead acid battery was released commercially [41-45].

These batteries are used for hybrid electric vehicles which follow the HRPSoC i.e. High Rate Partial State of Charge mechanism. In this application, the battery gets charged using regenerative brakes and the battery gets discharged at high rate while accelerating. Thus, it works at a partial state of charging. The main problem faced is that of accumulation of lead sulfate crystals in the negative plate while high rate discharging. There is rapid formation of lead sulfate crystals on reaction of spongy lead with electrolyte. This leads to the formation of a layer of lead sulfate which results in the low utilization of the negative active material. During charging process, more hydrogen gas is evolved by accepting electrons from the grid as it is overcharged and also water

loss takes place as a result of this continuous process [46-51]. The Sulfation in the negative plate under HRPSoC is presented in Fig.8.

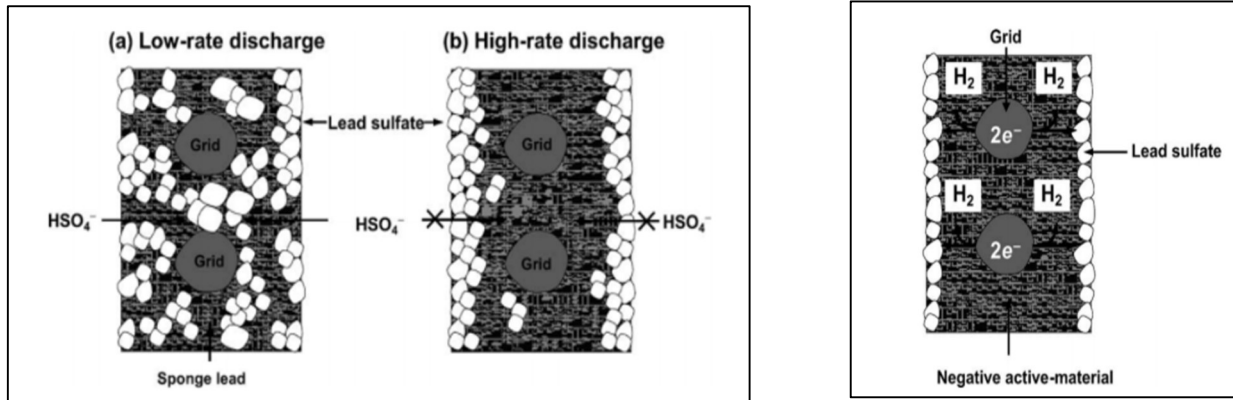


Figure 8: Problem of Sulfation in the negative plate under HRPSoC [56]

Many approaches have been tried to resolve these issues associated with these VRLA batteries. One of them is the addition of carbon compounds to the active material of the negative plate. Various types of carbon compounds have been added and their effects on the functioning and cyclability of lead acid batteries. The mechanism of the effect of carbon on the functioning of the negative electrode of the lead acid batteries has been studied widely.

The carbon compound that are added to the negative electrode should have the following characteristics [52-55]:

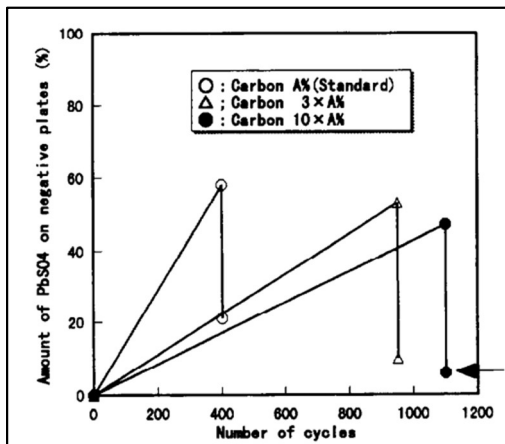
- 1) High electroconductivity: The carbon interphase should be electrochemically conducting, so that the electrochemical reactions of the battery can be carried out at the surface of the electrode where carbon is present.
- 2) High surface area: This feature should be present so that the porosity of the carbon compound is there and thus the process can only be achieved when nanosized particles are introduced.

3) Strong Adhesion to the lead particles: The strong adhesion of the carbon particles to the lead metal will ensure that the carbon will be in contact to the lead and there will be low ohmic resistance. Thus, the electrochemical reaction can take place at the interphase.

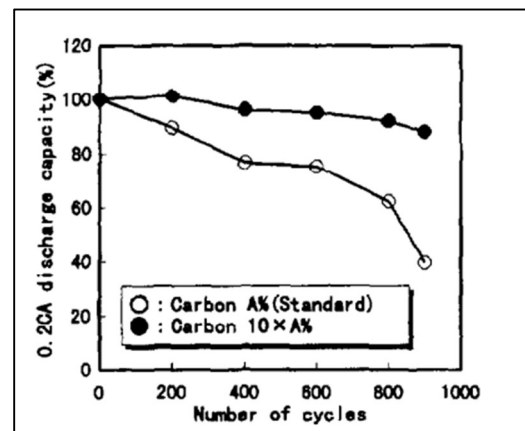
The effects that carbon has on these batteries can be summarized as follows:

Reduction in the amount of lead sulfate formed:

When carbon is added to the negative plate of a VRLA battery it is seen this that the loss in discharge capacity after certain cycles is lowered. The loss in the discharge capacity of the standard lead acid batteries is attributed to the fact that there is accumulation of larger lead sulfate crystal while discharging in HRPSoC application. Thus, it had been concluded that the negative plate in which carbon is added (Fig.9), the accumulation of lead sulfate is lesser in amount when compared to the conventional lead acid batteries.



(a)



(b)

Figure 9: (a) Effect of carbon as an additive on sulfation of negative plate (b) Effect of carbon on the discharge capacity of the battery @ C/5 rate

Particle size of lead sulfate crystals on the negative plate:

After cycling lead-acid batteries, lead sulfate layer in the negative electrode shows that the size of the PbSO_4 crystals is smaller for the negative electrode with more amount of carbon additive. This can be suggested that when only spongy lead is present in the negative electrode, the pores in the active material are larger in size. As a result of which larger crystals of lead sulfate are formed during the process of discharge. On addition of carbon as an additive for the negative electrode, the pores are filled and thus, the pore size is decreased. So, the lead sulfate that grows during the process of discharge are smaller and their dissolution while charging is easier. Thus, one of the problems of lead acid batteries i.e. the irreversible formation of lead sulfate can be reversed.

Conductivity of negative plates of lead acid batteries:

In a negative electrode with more amount of carbon compounds as additive contained carbon on and between the lead sulfate formed in the discharged negative plate. These carbon compounds provide a conducting network through the non-conducting solid crystals of lead sulfate (Fig. 10). This also allows the flow of electrons to the active material. So, while recharging the battery, more of the lead sulfate is converted back to lead and thus, reversibility is increased to higher extent. More amount of carbon introduces more conducting network and thus, dissolution of more amount of lead sulfate, hence more reversibility.

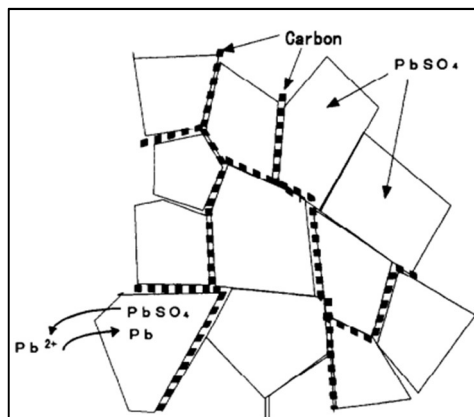


Figure 10: Schematic diagram of layering of Carbon on the negative plate

Lowering the overpotential of the negative electrode:

Addition of carbon into the negative electrode material lowers the electrode overpotential of the negative electrode. As a result of which the hydrogen evolution which occurs as a secondary inevitable reaction in the negative electrode is reduced. Hydrogen evolution and grid corrosion mechanism together contribute to the water loss. So, the water loss from the aqueous electrolyte of lead acid batteries can also be reduced [56-58].

Model for parallel mechanism of charging of a lead acid battery with carbon as a negative electrode additive:

The experimental data gave evidence for the fact that the addition of electrochemically active carbon compounds to the negative electrode of lead acid batteries lead to the increase in reversibility of the charge-discharge cycle of these batteries (Fig. 11). This in turn assured the longer life span of this batteries. A model can be used to explain the same.

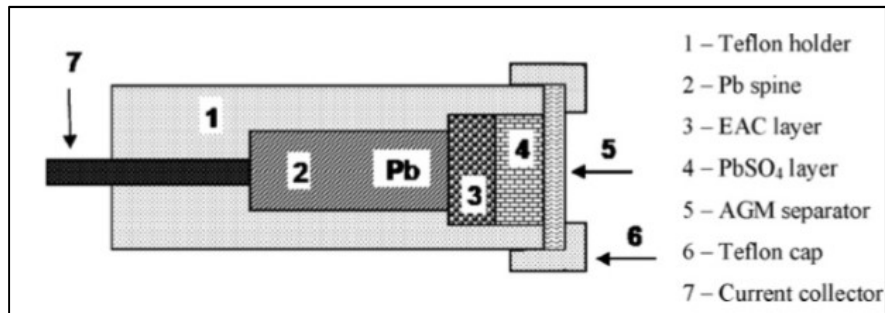


Figure 11: Schematic diagram of negative electrode with carbon additive

The factors that govern the difference in the charging rate and thus the reversibility of the lead sulfate solid crystals formed, charge transfer and reduction of Pb^{2+} ions.

During the charging process, the electrical double layer interface of both the lead/solution and carbon/solution interface are charged till a potential at which the reduction of adsorbed lead cations begin. The minimum potential required to cross the potential barrier for the reduction process depends on the nature of the interface. It had been observed that the potential at which the reduction process is carried out at the carbon surface is considerably lower as compared to that of potential required for the lead surface (Fig.12). The resistance of the lead/solution interface is higher and thus lesser flow of electron as compared to the carbon interface. The potential barrier which has to be crossed by the carbon/solution interface depend on the amount or concentration of carbon. As the potential barrier is low for carbon interface, thus the reduction process happens to be faster and thus more of lead sulfate is converted back to lead metal. The overpotential of reduction process is decreased for certain concentrations of the electrochemically active carbon. The electrode polarization depends on the ratio of lead to the carbon compounds in the active material [59-60].

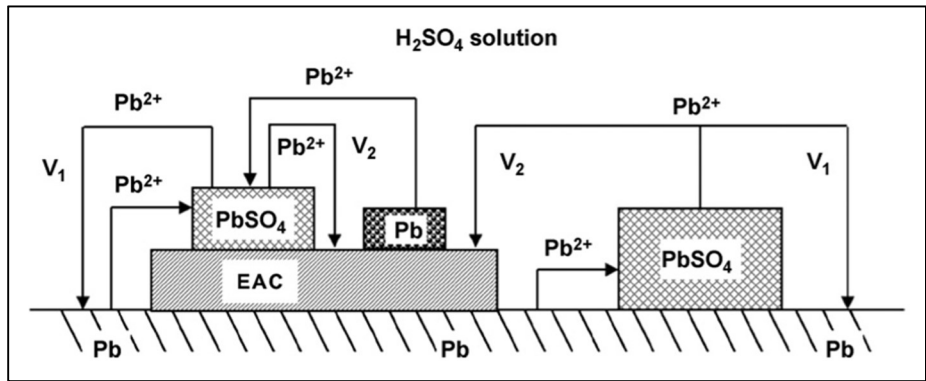


Figure 12: Mechanism in negative electrode with carbon additive

1.8. Various carbon compounds used as an additive:

Various kinds of carbon compounds have been used for the improvement in electrochemical performance of the lead acid batteries because of its beneficial effects mentioned earlier. The effect of various forms of carbon are illustrated below.

The addition of different compositions of carbon black to the negative active material of the battery was studied. The composition, particle size and purity of the carbon black additive governs the cycling performance. Minor amount of impurity does not cause much effect. Pure and ordered carbon black gave higher number of cycles and also higher cycling stability. This also enhanced the wetting of the battery plates and decreased the phenomenon of acid stratification. Thus, the time required for the acid mixing in flooded batteries decreased and hence the efficiency of the lead acid batteries [61].

Nanostructured carbon compounds are also introduced as an additive for lead acid battery and their performance under HRPSoC was observed. Thus, the effect of graphene, single walled carbon nanotube and multiwalled carbon tube on the cycling performance has been studied. The graphitic carbon provides a better cycle life because of its properties like high electronic conductivity as compared to other carbon compounds. The lead acid battery with graphene as an additive initially showed 1.65 Ah @ C/20 rate which was better than MWCNT and SWCNT but resulted in dying down of the battery after 2 cycle set of HRPSoC as compared to 5 and 7 cycle sets for SWCNT and MWCNT respectively. This was attributed to the fact that the graphene sheets decrease the pore size of the negative material such that the sulfate anions cannot penetrate and lead sulfate is not formed, instead a layer of PbO is formed [63, 65].

It was observed in a study that when heteroatom (example nitrogen, oxygen) enriched electrochemically activated carbon is used in place of pure carbon forms as an additive for the negative active material of a lead acid battery, the discharge capacity of the battery under HRPSOC application increased considerably. This is due to the induced higher porosity of the negative electrode material and thus enhances the cyclability [62].

Boron carbon nitride has also been studied as a negative electrode additive for the lead acid battery. It enhanced the performance of the battery under HRPSoC cycling. The pore size was reduced due to the filling of BCN in the plate. Thus, resulted in the formation of PbO instead of lead sulfate which hinders the contact of the active electrode material with the electrolyte i.e. aqueous sulfuric acid. It helps by disintegrating itself to carbon and nitrogen for better cycling [64].

So current research emphasis is given to develop high energy density (high performance) LABs with modified paste compositions, improve corrosion property of the positive plate, improve active material utilization of LAB.

The studies reported in the present thesis are confined to develop high performance lead-acid batteries through electrode additives which enhances battery performance, recyclability, formation efficiency, HRPSoC duty.

The present study

From the above review of literature on the LAB, developing high energy lead-acid batteries are essential. In this work we have studied the effect of boron doped graphene as an additive for negative electrode and studied its structural, Physical, electrochemical performance for lead acid battery.

References:

1. G. Planté, *C. R. Acad. Sci. Paris*, 1860, 50 640.
2. R. H. Newnham and W. G. A. Balasing, *J. Power Sources*, 66 (1997) 27.
3. Gaston Plante, *The Storage of Electrical Energy*, 1887
4. P. Whitehira, *J. Power Sources*, 42 (1993) 195.
5. P. Kurzweil, *J. Power Sources*, 14 (2010) 195, 4424-4434
6. J. Liu, *Adv. Funct. Mater.*, 2013, 23, 924–928
7. Bode H. *Lead Acid Batteries*, United States N. p., 1977
8. Linden. D. *Hand Book of Batteries and Fuel cells*, New York, McGraw-Hill Book Co., 1984
9. G.W Vinal *J. Optical Society of America*, 11 (1925) 3, 263-274
10. D. Norman Craig and G.W. Vinal *J. Research of the National Bureau of Standards*, 24, 1940
11. *A Guide to Lead Acid Battery* by ITACA
12. Vance H. Dodson *J. Electrochemical Soc.*, 108 (1961) 5, 406-412
13. R.V. Biagetti and M.C. Weeks *Bell Labs Technical Journal*, 49 (1970) 7
14. R. Biagetti *US Patent* 3,765,943, 1973
15. P. Ruetschi *J. Power Sources*, 2 (1977) 1, 3-120
16. S. Grugeon – Dewaele et al. *J. Power Sources*, 64 (1997) 71-80
17. Jeanne Burbank and Everett J. Ritchie *J. Electrochemical Soc.*, 110 (1969) 1, 125-130
18. D. Pavlov *Lead Acid Batteries: Science and Technology*, Elsevier, 2011
19. P. Ruetschi and R.T. Angstadt *J. Electrochem. Soc.*, 105 (1958) 10, 555-563
20. Kathryn R. Bullock and D. H. McClelland *J. Electrochem. Soc.*, 123 (1976) 3, 327-331

21. Kathryn R. Bullock and Edwin C. Laird J. Electrochem. Soc., 129 (1982) 7, 1393-1398
22. J. Garche J. Power Sources, 30 (1990) 1-4, 47-54
23. B. Calpin and D. A. J. Rand J. Power Sources, 36 (1991) 415-438
24. Kathryn R. Bullock J. Power Sources, 51 (1994) 1-2, 1-17
25. Rainer Wagner J. Power Sources, 53 (1995) 1, 153-162
26. K. Nakamura et al. J. Power Sources 59 (1996) 153-157
27. L.T. Lam et al. J. Power Sources, 133 (2004) 126–134
28. D. Pavlov et al. J. Power Sources 144 (2005) 521–527
29. Paul Ruetschi J. Power Sources 127 (2004) 33–44
30. H.A. Catherino et al. J. Power Sources 129 (2004) 113–120
31. The Grand View Research, February 2017
32. J.F. Manwell and J. G. McGowan Solar Energy, 50 (1993) 5, 399-405
33. C.D. Parker J. Power Sources, 100 (2001) 18–28 19
34. L.T. Lam, R. Louey J. Power Sources, 158 (2006) 1140–1148
35. K.C. Divya, J. Østergaard Electric Power Systems Research, 79 (2009) 511–520
36. J.B. Copetti and F. Chenlo J. Power Sources, 47 (1994) 109-118
37. M. Perrin et al. Journal of Power Sources, 144 (2005) 402–410
38. S. Sampath, D. D. Sarma, A. K. Shukla ACS Energy Lett., 2016, 1 (6) 1162–1164
39. W. B. Gu et al. J. Power Sources 108 (2002), 174-184
40. D. Berndt J. Power Sources, 100 (2001), 29-46
41. L. T. Lam et al. J. Power Sources, 174 (2007), 16-29
42. P.T. Moseley J. Power Sources 127 (2004) 27–32
43. M. Fernández et al. J. Power Sources 158 (2006) 1149–1165

44. A. Cooper, P.T. Moseley J. Power Sources 113 (2003) 200–208
45. V. Svoboda et al. J. Power Sources 144 (2005) 244–254
46. D. Pavlov et al. J. Power Sources, 113 (2003), 209-227
47. J. McDowall Power Engineering Society Summer Meeting, 3 (2000) 1538-1540
48. D.W.H. Lambert et al. J. Power Sources 107 (2002) 173–179
49. T. Ohmae et al. J. Power Sources 154 (2006) 523–529
50. M.L. Soria et al. J. Power Sources 168 (2007) 12–21
51. B. Hariprakash et al. J. Power Sources 191 (2009) 149–153
52. P.T. Moseley et al. J. Power Sources 174 (2007) 49–53
53. J.H. Yan et al. J. Power Sources 133 (2004) 135–140
54. P.T. Moseley et al. J. Power Sources 157 (2006) 3–10
55. D. Pavlov et al. J. Power Sources 191 (2009) 58–75
56. P.T. Moseley J. Power Sources 191 (2009) 134–138
57. K.R. Bullock J. Power Sources 195 (2010) 4513–4519
58. D. P. Boden et al. J. Power Sources 195 (2010) 4470–4493
59. M. Fernández et al. J. Power Sources 195 (2010) 4458–4469
60. J. Xiang et al. J. Power Sources 241 (2013) 150-158
61. E. Ebner et al. J. Power Sources 222 (2013) 554-560
62. K. Yang et al. J. Power Sources 239 (2013) 553-560
63. S. Mithin Kumar, S. Ambalavanan, Sundar Mayavan RSC Adv., 4 (2014) 36517 –36521
64. S. Mithin kumar, Uday Venkat Kiran, Arockia Kumar Raju, S. Ambalavanan and Sundar Mayavan RSC Adv., 1-2 (2012)
65. R. Marom et al. J. Power Sources 296 (2015) 78-85

66. T. B. Martins, R. H. Miwa, Antonio J. R. da Silva, and A. Fazio PRL 98, 196803 (2007)
67. Wang et al. J. Phys. Chem. C, 2013, 117 (44), pp 23251–23257

Chapter 2: Boron Doped Graphene as an Additive for Negative Electrode of High Performance Lead Acid Battery

2.1. Introduction to our approach: As discussed in Chapter I carbon addition in the negative electrode proves to be beneficial for the higher performance of advanced lead acid battery. Since this fact has been enlightened, various types of carbon compound and also carbon compounds mixed with different other hetero atoms and hetero compounds have been tried to improve the conductivity of battery paste. Most of the additions in this direction of research showed positive results.

Inspired by this logistics, we have chosen to use Boron Doped Graphene as an additive to the negative electrode of the Lead Acid Battery. The reasons behind choosing Boron Doped Graphene for the purpose of additive is given bellow:

Increases Conductivity: Graphene is conducting in nature. On doping graphene with Boron, a defect is introduced in the sheet type structure of graphene. The defect is due to the fact that Boron is trivalent in nature and carbon atoms embedded in the graphene nano sheets are tetravalent in nature. Thus, when some of the Carbons are replaced by Boron atoms in the process of doping, the valency of carbon atoms neighboring the boron atoms are not complete. Hence, holes are created and p-type conductivity is induced. In this way, a small band gap is introduced and semiconductor is produced. The B-doped graphene forms a electronically conductive network in the negative electrode and makes the process of charge-discharge easier [1-2].

Hence effect of electrochemical performance of Boron doped graphene additive to the negative active mass is worth investigating.

Various methods have been reported for the preparation of nano-structured Boron-Doped Graphene including Bottom Up as well as Top Down approaches. Top Down approach is one in which the nanostructured material is synthesized from a macro or micro material by some chemical or mechanical procedure of destruction, for example, Solid state synthesis, chemical methods, etc. Bottom Up approach is one in which the nanomaterials are synthesized from the scratch that is atomic or molecular level, for example, Chemical Vapour Deposition, Organic synthesis, co-precipitation, etc.

Boron Doped Graphene has been synthesized by using catalyst free- thermal annealing of Graphene oxide and B_2O_3 . Graphene can be prepared by arc discharge of graphite electrodes in presence of helium, hydrogen and diborane. Arc discharge method of Boron-packed Graphite electrode in presence of Hydrogen and Helium also gives boron doped graphene. Another Bottom Up approach involved the formation of Boron-Doped Graphene chemically using CCl_4 , BBr_3 and Potassium metal as reductant. BDG is also prepared by low pressure Chemical Vapour Deposition using phenylboronic acid as feedstock. It has also been reportedly synthesized by pyrolysis of graphene oxide and boric acid. Greener approach is also reported which involves reduction of GO using hydrogen to producing graphene [3-8].

In this course of investigation, Boron Doped Graphene is synthesized using a chemical method of exfoliation from Graphite powder and also Boric acid is used for the final step of formation of Boron Doped Graphene by Solvothermal method. This method involves three steps: (1) Synthesis of Graphene Oxide from Graphite powder, (2) Reduction of Graphene Oxide to Reduced Graphene Nanosheets and (3) Doping of Graphene Nanosheets with Boron using Boric acid

2.2 Chemicals and Reagents:

For Graphene Oxide Synthesis: 99.99% pure Graphite powder (China Steel Chemical Corporation, Taiwan), 98% H₂SO₄ (Finar), NaNO₃ (Avra Synthesis Pvt Ltd), KMnO₄ (Avra Synthesis limited), H₂O₂ (Avra Synthesis Pvt. Ltd.) and Distilled water was used.

For Synthesis of Boron Doped Graphene: Boric acid (Acros) and Ethanol (Merck) was used.

All the chemicals used are of analytical reagents grade and are used as received without any further purification. The aqueous solutions are prepared using distilled water.

2.3 Experimental procedure:

2.3.1. Synthesis of Graphene oxide from Graphite Powder using Modified Hummers'

Method:

0.5 g of Graphite powder and 0.5 g of Sodium nitrate (NaNO₃) was taken in a round bottom flask and mixed with 23 ml H₂SO₄ and stirred in ice bath for 4 hours. Then Potassium Permanganate (KMnO₄) was added slowly to the mixture by keeping the temperature still below 20° C in order to avoid unwanted overheating and explosion. The flask was then transferred to a temperature of 35°C and stirred for 2 hours. After that the mixture is cooled to a temperature below 20° C and 46 ml of distilled water is added. The mixture is stirred for 2 hours in oil bath which is already heated at 98°C. 100 ml of distilled water is then added to the mixture after cooling it to room temperature. This is then stirred at room temperature for 1 hour. After that 10 ml of H₂O₂ was added to the mixture and stirred for another hour and then transferred to a beaker using HCl- water mixture. It is washed several times till the supernatant solution turns clear. The supernatant solution is decanted and the mixture is dried to form the

powdery dark brown Graphene Oxide. Schematics of Synthesis of Graphene oxide from graphite precursor is presented in Fig. 13.

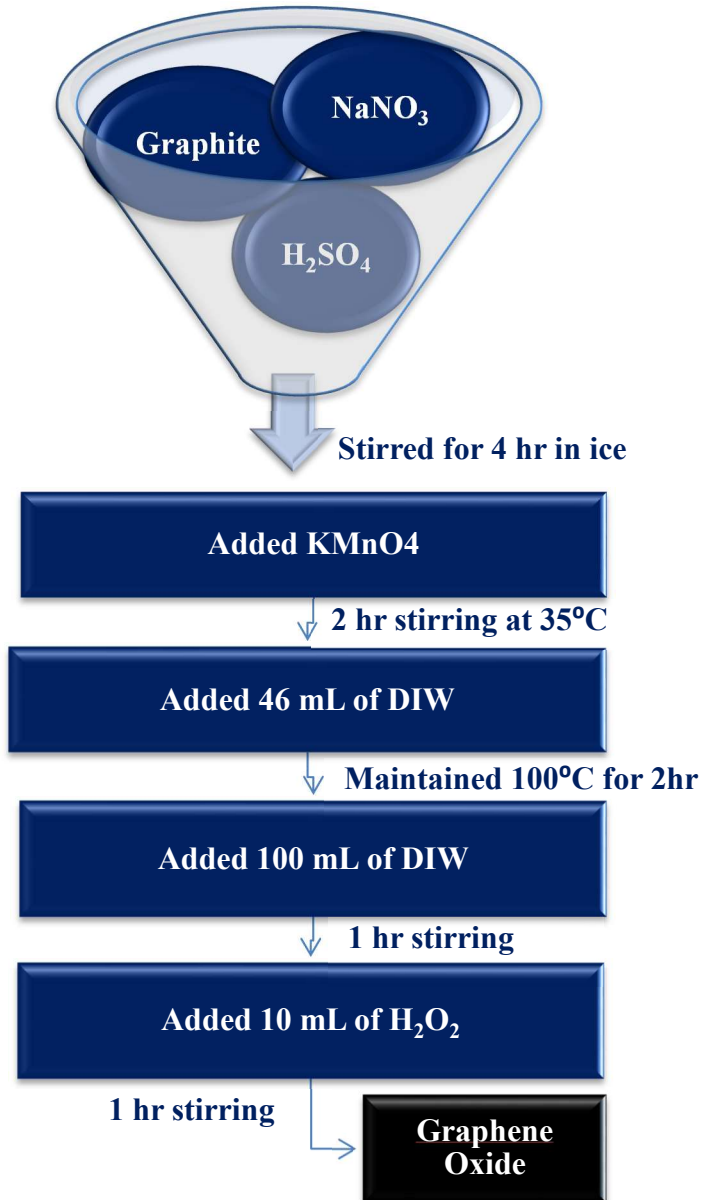


Figure 13: Schematics of Synthesis of Graphene oxide from graphite precursor.

2.3.2 Synthesis of T-GNS from Graphene Oxide:

Various chemical methods can be used for the reduction of Graphene oxide to Graphene Nanosheets. But here we employ the thermal method of reduction. 0.5g of Graphene oxide is taken in a quartz boat and heated in a tubular furnace at a temperature of 500° C in Argon atmosphere. Higher temperatures have been reported in literature for the same purpose but this moderate temperature is maintained in order to prevent the sample from agglomerating and thus, maintain the desired nanostructure of the sheets. The time given for the thermal reduction process is 20 minutes. The compound is then allowed to cool down at room temperature. A fine textured black Thermally reduced Graphene Nanosheets is formed.



2.3.3 Synthesis of Boron Doped Graphene from T-GNS:

The method used for the preparation of Boron Doped Graphene from T-GNS is a Solvothermal method using ethanol as a solvent. Schematic diagram of synthesis of Boron doped Graphene is presented in Fig. 14. Boric acid was taken as a source of Boron atoms for doping in the graphene sheets. 1.5 g of H₃BO₃ was taken in a beaker and mixed with 0.1 g of T-GNS with 50 ml of ethanol as solvent. The mixture was sonicated to dissolve all the solutes in the solvent. After the solution was homogenized properly, it was put into a Teflon sealed autoclave. The autoclave was then kept at 150°C for 12 hours. After that the autoclave was cooled to room temperature and the black powdered substance formed.

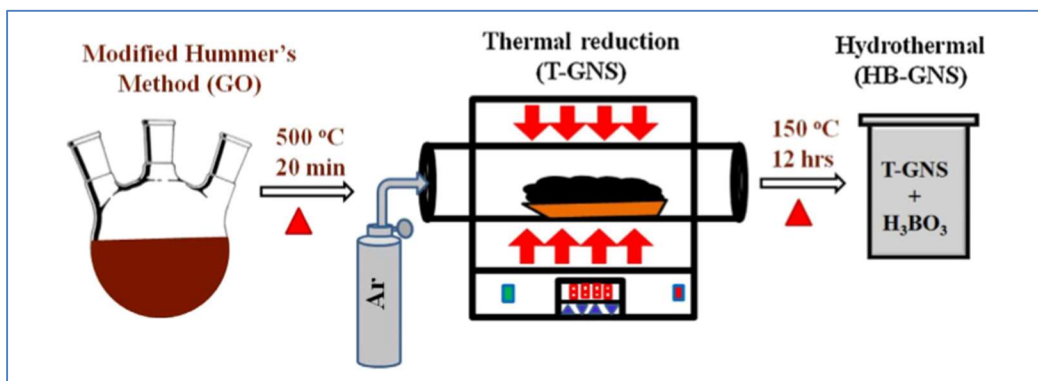


Figure 14: Schematic diagram of synthesis of Boron doped Graphene

This method is modified for various temperature and ratios of reactants to give different percentages of Boron doped in the graphene nano sheets. Their utility as an electrode additive was checked and thus the percentage of boron doping was optimized [9].

2.3.4. Structural and Physical Characterization:

The structure of the Boron doped graphene prepared by the above method was characterized using XRD (X-ray diffraction) study, XPS (X-ray Photoelectron Spectroscopy), SEM (Scanning Electron Microscopy) and TGA (Thermal Gravimetric Analysis).

XRD measurements of synthesized GO, T-GNS and B-GNS were performed using an AXS D8 Advance diffractometer (reflection $\theta - \theta$ geometry, Cu $K\alpha$ radiation, receiving slit of 0.2mm scintillation counter, 40mA, 40 kV) from Bruker Inc. (Germany). The diffraction data were collected at 0.0164 step size widths over a 2θ range from 10 to 100. The structural parameters were refined by Rietveld analysis that was performed with the TOPAS-3 program, which is a part of the Bruker software package.

The surface morphology of the powders were characterized by scanning electron microscope (JEOL-JEM-2011(200KV)).

X-ray photoelectron spectroscopy (XPS) used to determine the atomic percentages of boron, carbon and oxygen in the sample. X-ray photoelectron spectroscopy (XPS) measurements were carried out ESCA+, (Omicron nanotechnology, Oxford Instruments plc, Germany) equipped with monochromic AlK α (1486.6 eV) X-ray beam radiation operated at 15 kV and 20mA, binding energy was calibrated vs. carbon (C1s = 284.6 eV). For these measurements and characterization of sample, the powder samples were transferred to the XPS instrument device using a hermetically sealed unit, which contains a sample holder attached to a magnetic manipulator, and a gate valve. The spectra were deconvoluted using Gaussian functions based on Origin 8.0 software.

Thermal Gravimetric Analysis (TGA) used to determine the decomposition temperature of Boron Doped Graphene was carried out in TGA instrument SDT Q600 V20.9 Build 20 using Ramp method.

2.3.5 Fabrication and Assembly of battery electrodes:

The paste mix for the electrode was prepared with Lead Oxide, dynel fibers, barium sulfate, sulfuric acid, lignin and in this case different percentages of Boron Doped Graphene (0.25%, 0.5%, 0.75%, 1%). After thorough mixing of the paste, it is pasted onto the grids. This was followed by drying and then curing of the electrodes.

2V/2.1 Ah cells (Fig. 15) with different percentages of B-doped graphene (0.25%, 0.5%, 0.75% and 1%) as negative electrode additives were assembled by stacking two cured positive electrodes and one cured negative electrode. The cells assembled were negative limited. The negative and the positive electrodes were separated by Absorptive Glass Mat (AGM) separator. The plates were

tied using Teflon bands. The positive plates were soldered together to give the positive terminal of the cell and the negative plate was soldered to give the negative terminal of the cell. The assembly was then put into a polypropylene container. Before starting the process of formation, it was soaked in sufficient amount of 4.5 M H₂SO₄ to immerse the plates properly. It was then allowed a rest for 2 hours. The battery is then sealed using the lid of the container and Teflon.



Figure 15: A laboratory prepared lead acid cell with negative limited.

2.3.6 Electrochemical Characterizations:

The effect of Boron doped graphene as an additive for negative electrode material was studied by using various electrochemical characterizations like C-rate study, Cyclability, Linear Sweep Voltammetry and Simulated HRPSoC.

Linear Sweep Voltammetry: LSV experiment performed in the potential range -0.3 to -1.4 V. In the scan rate 5mV/s. The working electrode is the lead electrode (with conventional and B-GNS

additive, counter electrode is platinum foil and the reference electrode is Hg/ Hg₂SO₄/ 1.25 sp. gravity of H₂SO₄.

Cycling Studies: Initially, three formation cycles were completed at C/20 rate. Subsequently, cycling was performed at low to high rates i.e. C/10, C/5, C/2, 1C, 2C rates. After the different C – rate charge-discharge cycling, the cells were subjected to C/5 rate cycling using the constant current (CC) protocol.

Simulated HRPSOC: Different wt. % of boron doped graphene additive (0.25, 0.5, 1 wt. %) incorporated into the negative active mass (NAM) test cells were compared with the conventional cell in simulated High rate partial state of charge cycling (HRPSoC) conditions. In this experiment charge –discharge cycling occurs at the 4.2A. This experiment consists of the following steps. Charge at 4.2A (2C rate) for 1min, 10 sec rest, discharge at 4.2A (2C rate), 10 sec rest. This particular experiment was stopped when voltage reaches at 2.83V or when voltage fell down at 1.83V. This above process consists as the one cycle set. After completion of the one cycle set full recharged (SoC~1) with 20 hr. rate.

2.4. Results and Discussion:

2.4.1 Structural Characterization:

The phase characterization of Graphite, GO, RGO, T-GNS and B-GNS are done using X-ray Diffraction experiments. The XRD pattern for Graphite, GO and RGO are shown in the Figure 16 (a). Graphite shows a peak for the plane (002) at 2θ value of 26° . But for GO the 2θ value is decreased which signifies that the interlayer distance is increased which confirms the formation of GO. For RGO the number of sheets and also the functionalities are reduced, so the 2θ value is again increased. The XRD pattern for T-GNS and B-GNS are shown in the figure (b). The 2θ for

B-GNS is observed to be lower than that of T-GNS for the same plane (002). The peaks are not sharp as the samples are not crystalline solid.

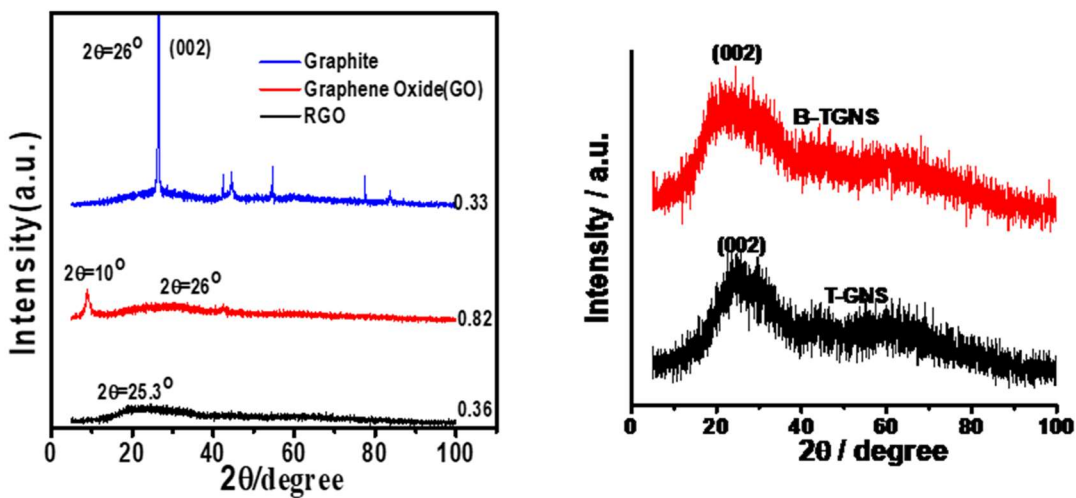


Figure 16: XRD of graphite, GO and RGO; and T-GNS and B-GNS

The slight decrease in the 2θ value for B-GNS indicates that there is little increase in the interlayer distance of B-GNS as compared to that of T-GNS. This may be attributed to the fact that Boron is a little bigger in size compared to carbon and hence increase in the interlayer distance and decrease in the 2θ value.

2.4.2 Morphology Studies:

The SEM images of Graphene Nanosheets are shown below in figure 17. The images show layered structure of the Graphene nanosheets and thus confirms the formation of nanostructured layered Thermally reduced graphene nanosheets (T-GNS).

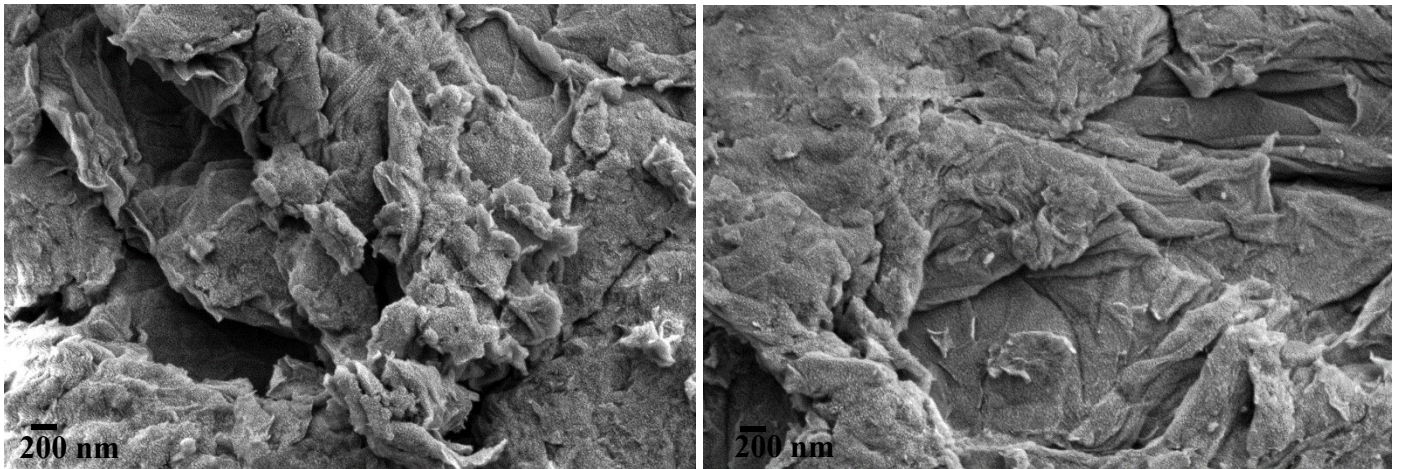


Figure 17: SEM images of Graphene Nanosheets

2.4.3 X-ray Photoelectron Spectroscopy:

B-GNS is characterized using XPS to understand the composition of the surface of the sample synthesized qualitatively as well as quantitatively. The XPS data plots are shown in the figure below. The graph is plotted with Binding Energy of the atoms vs the Intensity i.e. Counts per sec.

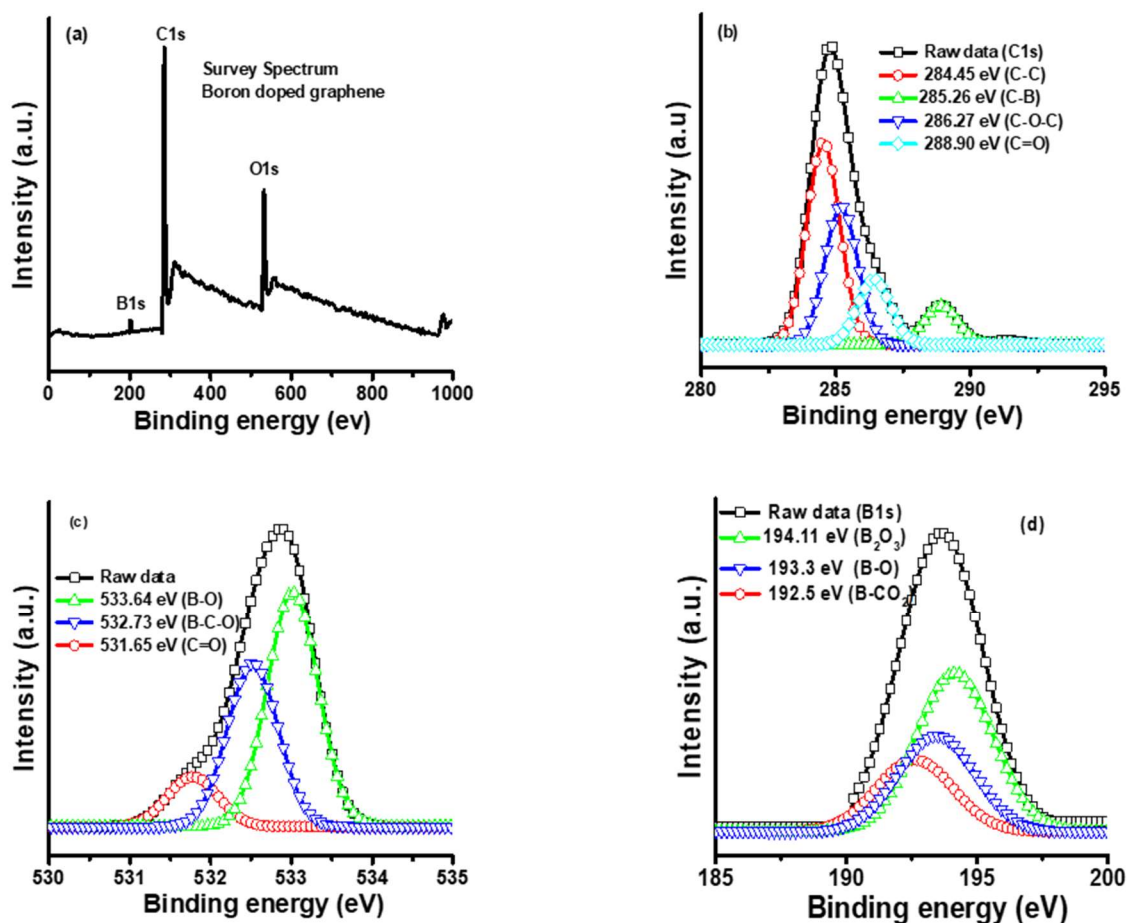


Figure 18: (a) Survey plot of XPS for B-GNS; XPS plot of (b) Carbon 1s (c) Oxygen 1s and (d) Boron 1s

The plot (a) shows a survey of the atoms present in the sample and also their quantities. The sample contains 83.67% C, 13.21% O and 3.11% B quantitatively. The figures (b, c and d) show the characteristic XPS BE curves for Carbon, Oxygen and Boron respectively. Each of the curves is constituted of the BE curves of various bonded forms of the same atom. The C1s plot shown in fig 18(b) shows peaks at 284.45eV for C-C; 285.4eV for C-B which confirms the incorporation of Boron in the graphene lattice; 286.27eV for C-O-C and 288.9 for C=O. The O1s plot shown in fig 18(c) shows peaks at 533.64eV for B-O; 532.7eV for B-C-O which reconfirms the presence of

Boron in the lattice and 531.65eV for C=O. The B1s plot in fig 18(d) shows peaks at 194.11eV for B_2O_3 ; 193.3eV for B-O and 192.5eV for B-CO₂ which confirms the doping.

2.4.6. Thermal Gravimetric Analysis:

TGA plot of Boron Doped Graphene is showed in the fig 19. It shows a decomposition at around 580°C which is slightly lower than the temperature of decomposition of Graphene Nanosheets which signifies that Boron Doped Graphene is slightly less stable thermally compared to Graphene nanosheets.

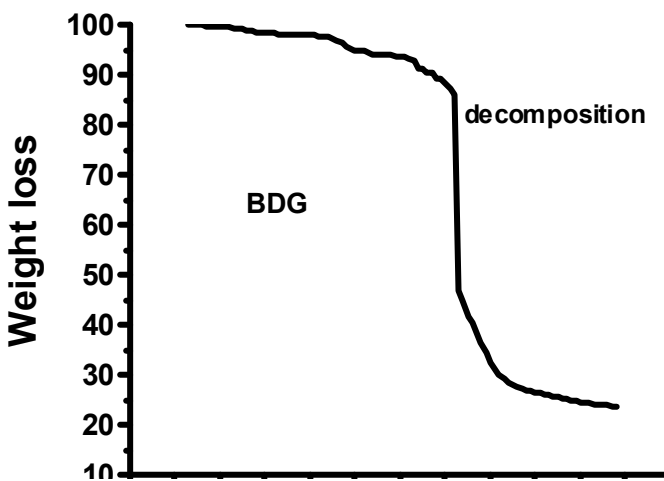


Figure 19: TGA plot for Boron Doped Graphene.

2.4.6 Electrochemical Characterization:

(a) Linear Sweep Voltammetry:

This is a current-voltage characteristic curve.

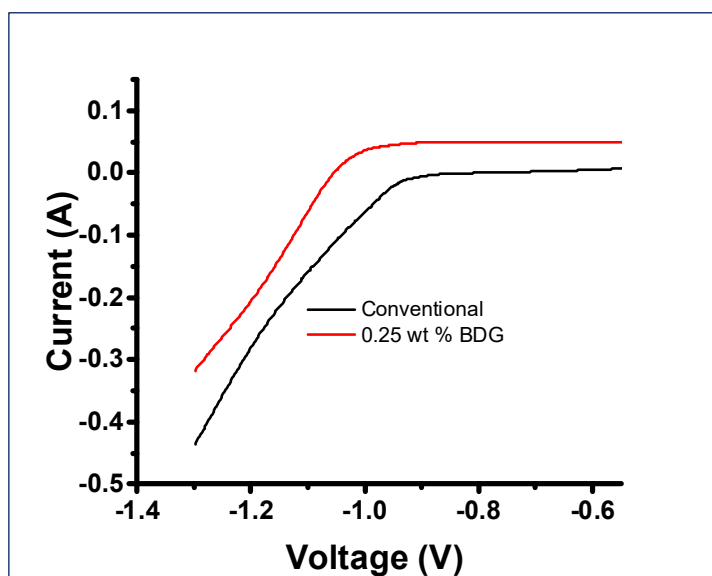
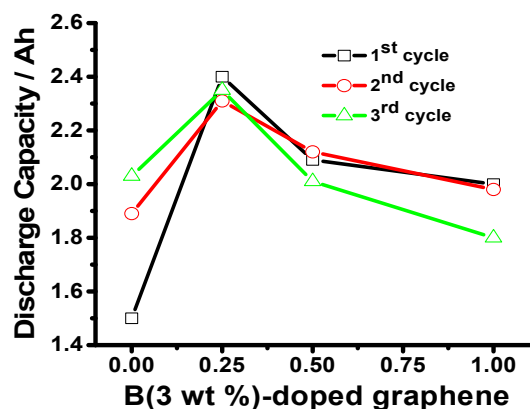


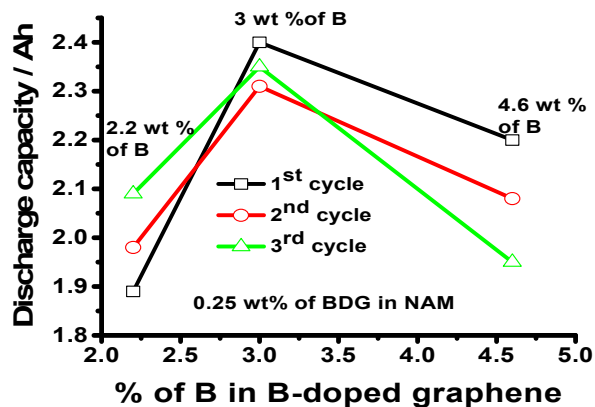
Figure 20: LSV plot of conventional and BGNS added negative electrode

This plot shows that at same voltage more current is passed through the electrode having 0.25% B-doped graphene additive. As more current is passed, more conductivity through the electrode and hence more conversion of lead sulfate (PbSO_4) to lead metal (Pb). Thus, the problem of irreversible sulfation in the electrodes is reduced.

(b). Initial capacity performance at 20 hr. rate:



(a)



(b)

Figure 21: (a) Study of formation cycle of the B (3%) doped GNS (b) Optimization of the % of B doping

The initial discharge capacity of B (3%) -doped graphene (0, 0.25, 0.5 and 1 wt. %) additives were determined by 20 hr. rate performance. Discharge capacity mainly depends on the utilization of negative active mass in negative plate. To characterize the initial discharge capacity test performed by the 3 cycles at 20 hr. rate at room temperature. Standard requirement of the initial capacity test was to get more than full capacity in the first cycle at C/20 rate. Different weight percentages of B(3%) -doped graphene additive shows the full capacity in the first cycle compared without additive cell. 0.25 wt. % of B (3%) -doped graphene additive cell shows the capacity > 80 % compare to the without additive cell. 0.5, 1 wt. % of the B (3%) -doped graphene additive shows percentage increases the > 50, 60 % respectively. Fig: 21 (b) Results indicates that increase in weight percentage of the additive shows the diminish the capacity of the cell.

We have optimized the different percentages of boron in B-doped graphene in negative active mass i.e., 2.2, 3% and 4.6 % of boron. These experimental outcomes specify the optimum percentage of boron is 3% in B-doped graphene. B(3%)- doped graphene delivers highest capacity compared to the other additives.

(c) C-Rate Study and C/5 rate cycling:

The cells with different percentages of the electrode additive are studied at different C-rates i.e., C/10, C/5, C/2, 1C, 2C. It was seen as in fig. 22 that the optimum percentage of Boron (3%) doped graphene shows the better result at all the C-rates compared to the other additives. The increase in capacity for lower C-rates is about 20% but for higher C- rates the increase in capacity is almost doubled.

Electrochemical cyclic stability of as prepared boron doped graphene in negative active material calculated by the galvanostatic charge- discharge cycling at C/5 rate. For comparison, we also show the performance of different content of additives in the negative active material. Enhanced cycling stability of the cell is due to the boron doped graphene in the negative active material is ascribed to favor the charge storage. More charge storage based on the electron deficiency of boron i.e., it acts a capacitor. By this approach it decreases the lead sulphate crystal formation in negative plate. At C/5 rate it shows more stable discharge capacity till around 150 cycles of the cell. The discharge capacity is stable for the optimum boron doping condition i.e. 3% in the negative electrode additive. It shows an increase in the discharge capacity by almost 15% in comparison to the conventional cell.

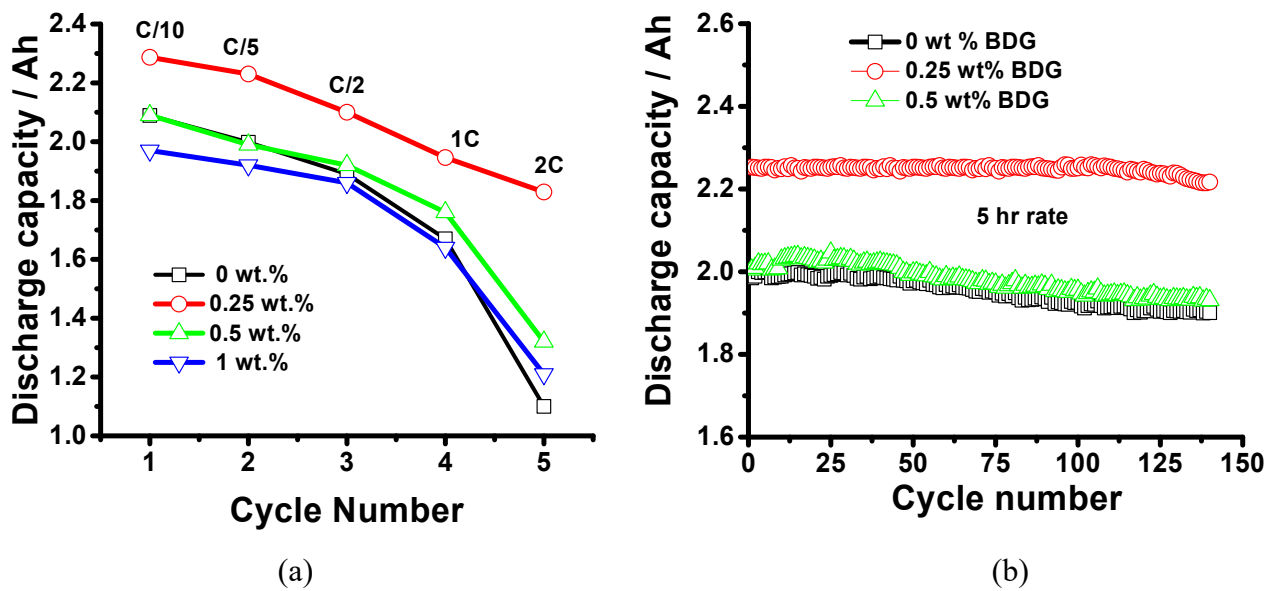


Figure 22: (a) C-Rate performance Study of batteries with different percentages of BDG as electrode additive (b) Cycling Stability at C/5 rate of Lead acid batteries with different percentages of BDG as electrode additive.

(d) High rate partial state of charge cycling (HRPSoC) study

Based on the results we concluded that cycling with high rate partial state of charging in conventional cell gives the 6112 cycles, whereas additive cell shows the longer cycle life. Fig: 22 (a) explains the conventional cell shows the lower cycle life compared to the additive cell, due to the harsh cycling occurs at the surface of the negative plate. More formation of the lead sulphate at the negative plate surface. Fig 22 (b): 0.25 wt% of BDG additive cell shows the 11500 cycles whereas conventional cell shows the 6112 cycles. 0.25 wt% BDG additive two times more cycle life compared to the conventional cell. Fig 22(c, d) : shows the 0.5, 1 wt% of additive shows the less cycle life compare to the 0.25 wt% of additive. As the BDG % increases in the negative active mass shows the negative effect to the capacity in the cell. 0.5 and 1 wt% of BDG additive shows the 8219, 8584 cycles respectively and compare to conventional cell ~30 % improvement in the

cycle life. Based on the results we confirmed the B-doped graphene acts as a charge storage (Capacitor), because of the electron deficient nature of the boron.

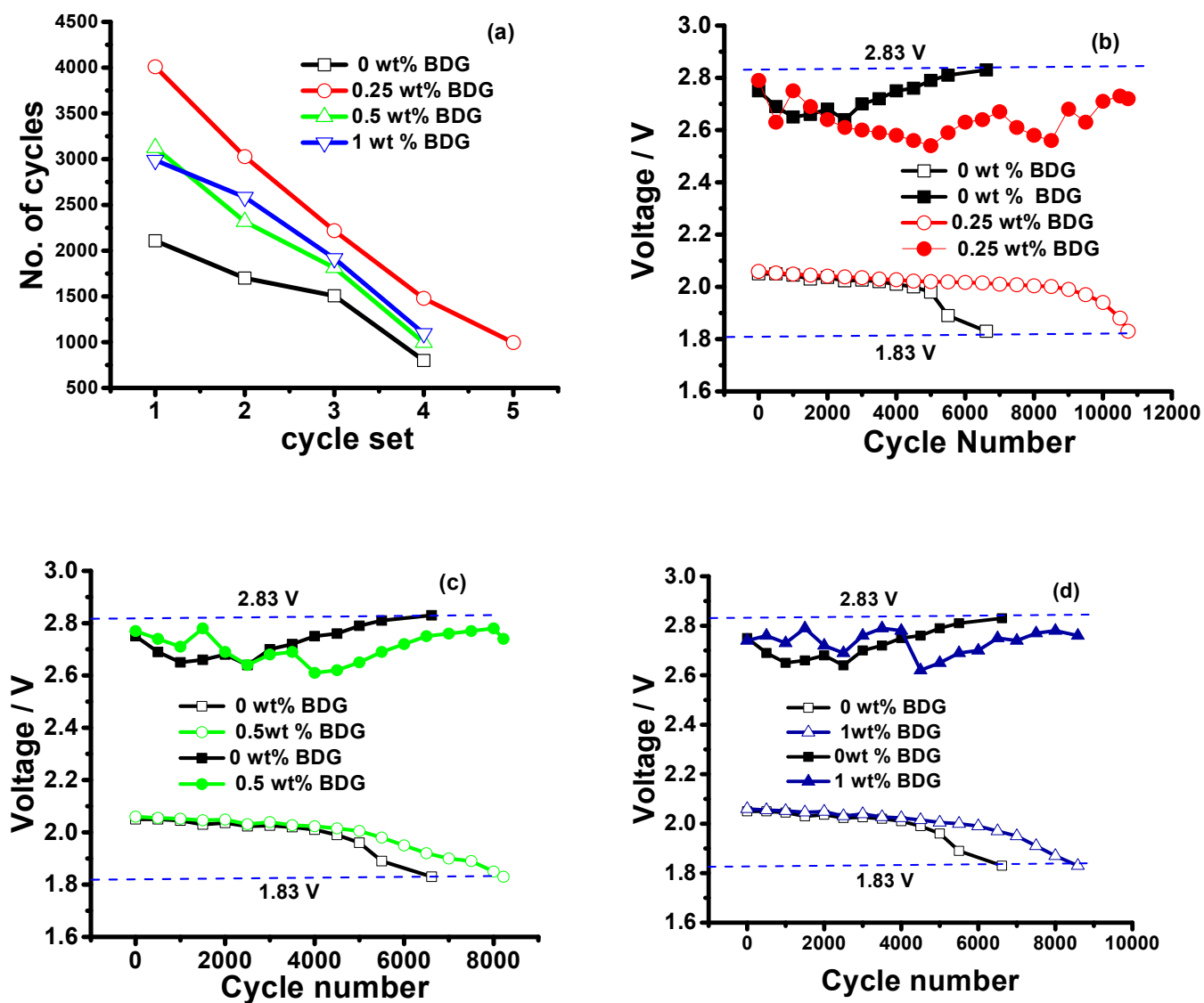


Figure 22: (a) Comparison of various B-doped graphene additive and conventional cell cycle set w.r.t. cycle number. Fig: (b, c and d) shows the end of charge and end of discharge voltages during the high rate partial state of charge cycling at 4.2 A.

Summary of the work:

We have successfully synthesized Boron doped Graphene using three steps. First step being the chemical exfoliation of Graphite precursor to give Graphene Oxide (GO) using modified Hummers Method. In the second step, GO is converted to Thermally Reduced Graphene Nanosheets (T-GNS) by Thermal reduction in a tubular furnace. Finally, Boron doped Graphene was synthesized using Solvothermal synthesis of T-GNS, H_3BO_3 (source for Boron) and using ethanol as solvent. The structure of B-GNS and the intermediates prepared were characterized using X-ray Diffraction studies. The surface morphology of the compounds synthesized were characterized using Scanning Electron Microscopy. The qualitative as well as quantitative composition of the B-GNS prepared was found out using X-ray Photoelectron Spectroscopy. The B-GNS sample was further characterized using TGA. The B-GNS was added to the negative electrode paste in different percentages (0.25%, 0.5%, 0.75% and 1%) and the electrodes were fabricated and assembled to for a negative limited battery. Additives with different percentages of doping were also analyzed. The electrochemical performance of the battery was tested using LSV, C-rate study and cycling stability @C/5 rate. It was found that the battery with 0.25% of Boron (3.11%) – doped graphene showed the optimum discharge capacity in the formation cycle and also better cycling stability. At lower C-rates, the discharge capacity was increased by 15-20% as compared to conventional but at higher C-rates, the capacity was almost doubled. High Rate Partial State of Charge cycling was performed and the battery with 0.25% of B (3%)- doped graphene additive exhibited twice the number of cycles compared to conventional lead acid battery. Thus, Boron Doped Graphene can be considered to be a potential negative electrode additive used in optimum quantities as investigated in this study.

References:

1. Stefano Agnoli and Marco Favaro *J. Mater. Chem. A*, 2016, 4, 5002–5025
2. Sugata Mukherjee and T.P. Kaloni *J. Nanopart Res* (2012) 14:1059
3. Zhen-Huan Sheng, Hong-Li Gao, Wen-Jing Bao, Feng-Bin Wang and Xing-Hua Xia *J. Mater. Chem.*, 22 (2012), 390-395
4. By L. S. Panchakarla, K. S. Subrahmanyam, S. K. Saha, Achutharao Govindaraj, H. R. Krishnamurthy, U. V. Waghmare and C. N. R. Rao *Adv. Mater.* 21 (2009), 4726–4730
5. Tianquan Lin, Fuqiang Huang, Jun Liang and Yingxia Wang *Energy Environ. Sci.*, 4 (2011), 862-865
6. Huan Wang, Yu Zhou, Di W, Lei Liao, Shuli Zhao, Hailin Peng, and Zhongfan Liu *Small* 8 (2013) 9, 1316–1320
7. L. Niu et al. *Electrochim. Acta* 108 (2013) 666–673
8. M. Sahoo et al. *Materials Research Bulletin* 61 (2015) 383–390
9. V. Thirumal et al. *Synthetic Metals* 220 (2016), 524–532